JOURNAL OF GEOPHYSICAL RESEARCH, VOL. 103, NO. D7, PAGES 8341–8353, APRIL 20, 1998

Processes controlling dimethylsulfide over the ocean: Case studies using a 3-D model driven by assimilated meteorological fields

Mian Chin,[1,2] Richard B. Rood,[3] Dale J. Allen,[4] Meinrat O. Andreae,[5] Anne M. Thompson,[3] Shian-Jiann Lin,[6] Robert M. Atlas,[3] and Joseph V. Ardizzone[7]

Abstract. This study investigates the processes that influence dimethylsulfide (DMS) concentrations over the ocean using a global three-dimensional chemistry and transport model (CTM). The model is driven by assimilated meteorological data from the Goddard Earth Observing System Data Assimilation System (GEOS-1 DAS). Results from the model are compared with DMS measurements from two marine sites, a ship cruise, and an aircraft campaign. When observed seawater DMS concentrations and meteorological conditions are used, the model reproduces the observed daily and diurnal variations of DMS concentrations at a tropical Pacific station. The model also predicts the observed changes of DMS concentrations across the Atlantic, although it overestimates the DMS level by a factor of 2. The calculated vertical DMS concentrations off Tasmania are more than 4 times higher than the measured data. The model simulates day-to-day fluctuations and interannual variations observed at Amsterdam Island but underpredicts the magnitude of the variations. Sensitivities for DMS concentrations to the parameters used in DMS emission, oxidation, boundary layer mixing, and cloud convective transport are tested. The limitations of the current model in interpreting the observations are due to (1) the uncertainties in parameterization of DMS emission from the ocean, (2) the simplistic boundary layer mixing scheme, (3) the inaccurate spatial distribution and intensity of deep convective clouds in the GEOS-1 DAS, and (4) the uncertainties in DMS oxidation rates.

1. Introduction

Dimethylsulfide (DMS, CH_3SCH_3) is the most important biogenic sulfur gas in the atmosphere. DMS is produced in seawater by marine phytoplankton, and it diffuses from the sea surface to the atmosphere, where it is oxidized to sulfate aerosol with a lifetime of one to a few days. Emission of DMS from the ocean accounts for 20–30% of the total sulfur emission according to current emission inventories [*Spiro et al.*, 1992; *Benkovitz et al.*, 1996; *Chin et al.*, 1996]. Unlike the anthropogenic sulfur sources, which are concentrated in the northern hemispheric midlatitude continents, DMS has widespread sources over the oceans around the world. Because it is the predominant source of sulfate aerosol over the remote ocean and perhaps in the tropical free troposphere [*Chatfield and Crutzen*, 1984; *Chin and Jacob*, 1996], DMS plays an important role in radiative forcing and, consequently, in global climate [*Charlson et al.*, 1987].

Concentrations of atmospheric DMS have been measured in many field observations. The majority of the data were collected over relatively short time periods (several days to several weeks) in aircraft campaigns or ship cruises. To assess the role of different processes (emission, transport, chemistry) that control DMS concentrations, models ranging in complexity from zero-dimensional box models to three-dimensional (3-D) chemistry transport models have been used [e.g., *Yvon et al.*, 1996; *Suhre et al.*, 1995; *Langner and Rodhe*, 1991; *Pham et al.*, 1995; *Feichter et al.*, 1996; *Chin et al.*, 1996]. The 3-D models have the advantage that the transport processes are governed by explicitly predicted atmospheric circulation, compared to the simple models in which the transport processes are often highly parameterized. However, previous 3-D models have been driven either by general circulation models or by monthly mean winds and hence are climatological in nature. It is therefore often difficult to apply such a model to the interpretation of the observed DMS concentrations measured in short-term observations.

Here we present a 3-D model simulation of atmospheric DMS using assimilated meteorological data. The NASA Goddard Earth Observing System version 1 Data Assimilation System (GEOS-1 DAS) generated meteorological fields [*Schubert et al.*, 1993] are used to drive a global 3-D chemistry and transport model (GEOS CTM). The GEOS-1 DAS product is currently available from January 1980 through December 1994. It contains a number of diagnostic fields for chemistry transport model applications. The main advantage of the as-

[1]Universities Space Research Association, NASA Goddard Space Flight Center, Greenbelt, Maryland.
[2]School of Earth and Atmospheric Sciences, Georgia Tech, Atlanta.
[3]NASA Goddard Space Flight Center, Greenbelt, Maryland.
[4]Department of Meteorology, University of Maryland, College Park.
[5]Biogeochemistry Department, Max Planck Institute for Chemistry, Mainz, Germany.
[6]Joint Center for Earth System Technology, University of Maryland at Baltimore County, NASA Goddard Space Flight Center, Greenbelt.
[7]General Sciences Corporation, NASA Goddard Space Flight Center, Greenbelt, Maryland.

Paper number 98JD00107.
0148-0227/98/98JD-00107$09.00

Table 1. GEOS-1 DAS Meteorological Fields Used as Model Input

Variable	Time Resolution
Surface pressure	6 hours, instantaneous
Temperature	6 hours, instantaneous
Wind velocity	6 hours, instantaneous
Cloud mass flux	6 hours, averaged
Detrainment	6 hours, averaged
Boundary layer thickness	3 hours, averaged
Wind velocity at 10 m	
Land	3 hours, averaged
Ocean[1]	6 hours, instantaneous

[1] From SSM/I observations; see text for explanation.

similated meteorological data driven CTM, compared to the GCM driven CTM, is that species concentrations can be simulated for the time period when observations are made; therefore it is particularly suited for case studies. The GEOS CTM has recently been applied to simulations of ^{222}Rn [*Allen et al.*, 1996a] and CO [*Allen et al.*, 1996b]. It is found that day-to-day and year-to-year variations of observed ^{222}Rn and CO at the North Atlantic sites are reproduced by the model and that transport-induced interannual variability explains approximately 80% of total interannual variability of CO at these sites [*Allen et al.*, 1996b]. It has been indicated that assimilated data can be used to remove meteorological variability, thus allowing more meaningful interpretation of the observed tracer concentrations [*Allen et al.*, 1996a].

We report in this paper four case studies using the GEOS CTM in order to examine the model's ability to simulate spatial and temporal variations in DMS concentrations and to determine the sensitivity of DMS levels to the uncertainties in emission, chemistry, and vertical mixing processes in the model. Model results are compared with observations at two marine surface sites, from a ship cruise, and from an aircraft campaign. We want to point out, however, that the purpose of this work is not to provide DMS distributions and budget on a global scale, but rather to evaluate the physical and chemical parameters in the model and to determine the ways to reduce the model uncertainties. This work is the first step toward our comprehensive study of the tropospheric sulfur cycle using the GEOS CTM.

2. Model

The configuration of the GEOS CTM used in this study has a horizontal resolution of 2° latitude by 2.5° longitude and 20 vertical sigma layers extending from the surface to 10 mbar, with the five lowest layers centered approximately 50, 250, 600, 1100, and 1800 m above the surface. The meteorological fields used to drive the off-line CTM are assimilated data from the GEOS-1 DAS. Upper air quantities are saved every 6 hours, and selected surface fields are saved every 3 hours [*Schubert et al.*, 1993]. Table 1 lists the meteorological fields used as model input. The instantaneous meteorological fields are interpolated to the CTM time (with a time step of 15 min).

The continuity equation for DMS is solved for mixing ratio changes resulting from emission, chemistry, advection, boundary layer mixing, and moist convective processes. The advection, boundary layer mixing, and convection schemes in the GEOS CTM have been described in detail by *Allen et al.* [1996a]. The following is a brief summary. Advection is computed by a flux-form semi-Lagrangian method [*Lin and Rood*, 1996; *Lin et al.*, 1994]. Moist convection is calculated using archived cloud mass flux fields from the GEOS-1 DAS. Boundary layer turbulent mixing in the model is parameterized such that a fraction (α) of material in each model layer within the boundary layer is mixed uniformly throughout the boundary layer. The boundary layer depth (defined as the difference between the pressure at the surface and the pressure at the altitude at which the turbulent kinetic energy reduces to 10% of its surface value [*Takacs et al.*, 1994]) is obtained from the GEOS-1 DAS. The parameter α can vary from 0 for an unmixed boundary layer to 1 for a completely mixed boundary layer. A disadvantage of this boundary layer mixing parameterization is that the value of α is not derived from physical considerations and α does not adequately represent the complexity of the boundary layer. Above the boundary layer, the results are not sensitive to the specification of α. However, concentrations within the boundary layer are strongly affected by the choice of α [*Allen et al.*, 1996a]. We assume a partially mixed boundary layer with $\alpha = 0.3$ in our standard simulation.

The DMS emission algorithm and chemistry are adapted from the study of *Chin et al.* [1996]. Oceanic DMS emission is computed as a product of the seawater DMS concentration and sea-to-air transfer velocity. Seawater DMS concentrations are specified as a function of latitude (and longitude in the tropics) for a winter and summer season [*Bates et al.*, 1987]. We impose a sinusoidal function constrained by the winter/summer average values to model the seasonal variation of the seawater DMS concentration. The transfer velocity of DMS is computed from that of CO_2, which is assumed to be linearly proportional to the 10-m wind speed for winds stronger than 3 m s^{-1} [*Tans et al.*, 1990]. It is noted that there are large uncertainties in the relationship between the wind speed and transfer velocity; for example, different algorithms describing this relationship [e.g., *Smethie et al.*, 1985; *Liss and Merlivat*, 1986; *Wanninkhof*, 1992; *Erickson*, 1993] can result in a factor of 2 or more difference in calculated transfer velocity at a given wind speed. Figure 1 shows the DMS transfer velocities at 20°C calculated from Tans et al., Wanninkhof, and Liss and Merlivat algorithms. We chose the *Tans et al.* [1990] algorithm because it produces a DMS source which was found in a previous global model study to be consistent with sulfate (a final product of DMS oxidation) concentrations at remote oceanic sites [*Chin et al.*, 1996]. The 10-m winds over the ocean retrieved from satellite observations by the special sensor microwave imagers (SSM/I) are used instead of the GEOS-1 DAS 10-m winds for calculating the DMS emission. SSM/I winds have been validated against observations and found to give an accurate representation of both wind speed and direction [*Atlas et al.*, 1996]. As we will show in the next section, the SSM/I winds agree with the local measurements better than GEOS-1 DAS 10-m winds in all case studies. The SSM/I instruments were operated on a series of Defense Meteorological Satellite Program satellites and have provided surface wind speeds over the global oceans from July 1987 to the present [*Atlas et al.*, 1996]. The gridded (2° × 2.5°) instantaneous SSM/I winds with a frequency of 6 hours that were generated by *Atlas et al.* [1996] are interpolated to the CTM time.

The oxidation of DMS includes reaction of DMS with OH during the day and with NO_3 at night. Concentrations of 5-day average OH are taken from *Spivakovsky et al.* [1990]. They were generated in a 3-D model simulation of methylchloroform under meteorological conditions of the general circula-

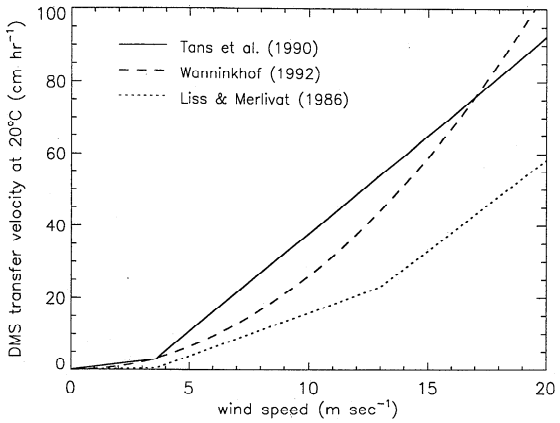

Figure 1. Transfer velocity of DMS at 20°C calculated using air-sea exchange algorithms from *Tans et al.* [1990] (solid line), *Wanninkhof* [1992] (dashed line), and *Liss and Merlivat* [1986] (dotted line). The explicit relationship between the wind speed and CO_2 transfer velocity of *Tans et al.* [1990] was given by *Erickson* [1993] for wind speed >3.6 m s^{-1}, and we assume a small value of transfer velocity at wind speed <3.6 m s^{-1}.

tion model from Goddard Institute of Space Studies (GISS GCM). Variations of OH during the day are obtained by scaling the average values to the cosine of the solar zenith angle. Oxidation of DMS by NO_3 at night is assumed to be limited by the rate of NO_3 production from the $NO_2 + O_3$ reaction, with NO_2 and O_3 fields compiled by *Spivakovsky et al.* [1990]. Concentrations of OH, NO_2, and O_3 are then interpolated to the GEOS CTM pressure levels. Several field studies of the sulfur budget in the marine boundary layer have indicated that DMS is oxidized faster than expected from reactions with OH and NO_3 [e.g., *Suhre et al.*, 1995; *Yvon et al.*, 1996]. It has been found in a global sulfur model simulation that the DMS oxidation rate has to be doubled in order to reproduce the observed concentrations of DMS and its final product sulfate at remote marine sites [*Chin et al.*, 1996]. The need for increasing the DMS oxidation rate in the model suggests that either OH and/or NO_3 concentrations in the model are too low, reported DMS reaction rate coefficients are too low, or there may be an important unknown DMS oxidant or oxidation pathway. Here we assume a factor of 2 increase in the DMS reaction rates with OH and NO_3 in the standard simulation, following *Chin et al.* [1996].

The simulations start from a low DMS initial concentration (0.1 parts per trillion by mole, or ppt), and the first 7–10 days are used for initialization of the troposphere.

3. Results

We focus on the comparison of model simulations with DMS measurements in four cases: (1) 1 week of surface measurements at a tropical Pacific station [*Yvon et al.*, 1996], (2) 50-day ship cruise measurements across the tropical Atlantic Ocean [*Andreae et al.*, 1994, 1995; *Suhre et al.*, 1995], (3) 1 week of vertical profile measurements off Tasmania near Cape Grim in the southern Pacific [*Berresheim et al.*, 1990], and (4) two consecutive summer season measurements at Amsterdam Island in the southern Indian Ocean [*Putaud et al.*, 1992]. These diverse cases provide a test of the model's ability to simulate daily and diurnal variations, the vertical distributions, and the interannual differences of DMS. The observations in the first two cases also include meteorological data such as wind speed and radiosonde observations that are useful for comparison with the prediction of 10-m wind speed and boundary layer height in the model. It should be pointed out that since the locations of the measurements are in the tropics and in the southern hemisphere, where meteorological input into the GEOS-1 DAS is relatively sparse, these simulations are a difficult test of the quality of the GEOS-1 DAS meteorological fields. It has been shown in the previous GEOS CTM studies that northern hemispheric simulations of tracer behavior were of consistently better quality than tropical or southern hemispheric tracer simulations [*Allen et al.*, 1996a, b].

3.1. DMS at a Tropical South Pacific Station (Case 1)

Concentrations of DMS in surface air at an oceanographic station located in the tropical South Pacific Ocean (12°S, 135°W) were measured together with seawater DMS concentrations and meteorological conditions in March 3–10, 1992, during the International Global Atmospheric Chemistry/Marine Aerosols and Gases Experiment [*Yvon et al.*, 1996]. The average value of observed seawater DMS concentration was 4.1 nmol L^{-1}, which was much higher than the previously reported values of 2.4 nmol L^{-1} for the global mean seawater concentration in tropical oligotrophic waters [*Andreae*, 1990], and 0.91–1.38 nmol L^{-1} at a nearby location for the same season of the year [*Bates et al.*, 1987]. The model "default" value of seawater DMS for the grid cell containing the measurement station is 1.90 nmol L^{-1}. To have a meaningful comparison between the model results and observations, we used the measured seawater DMS concentration for the vicinity area (1.5×10^6 km^2) around the station to calculate the DMS emission.

Seawater DMS concentrations and 10-m wind speeds from SSM/I used as model input are shown in Figures 2a and 2b, respectively. Also shown in Figure 2b are the 10-m winds from the GEOS-1 DAS as well as that measured at the station. The SSM/I 10-m winds aptly track the locally measured winds, although they cannot capture the small-scale variations because of the relatively coarse time resolution (6 hours). In comparison, the GEOS-1 DAS 10-m winds are approximately 20% lower than the observed values before March 9 and about 50% lower on March 9. The calculated DMS emission rates, as a function of seawater DMS concentrations and the SSM/I 10-m wind speeds, are between 10 and 30 μmol m^{-2} d^{-1}, with a mean value of 21 μmol m^{-2} d^{-1} (Figure 2c). Figure 2d shows that the calculated surface air DMS concentrations (mean 293 ppt) are about a factor of 1.6 lower than the observed concentrations (mean 454 ppt).

Possible explanations for the low bias in the model are that the DMS emission rate is too low, the DMS oxidation rate is too high, boundary layer mixing is too strong, or cloud convective transport is excessive. We have calculated the sensitivity of DMS concentrations to the variations of parameters in these processes; the results are shown in Figure 3. Surface DMS concentrations respond linearly to the emission rates; when the emission rates are increased by a factor of 1.6, DMS concentrations rise by about the same factor (Figure 3a). It should be borne in mind that the sea-to-air transfer algorithm use in our standard simulation already generates higher DMS emission rates than other algorithms in the literature (Figure 1); a factor of 1.6 increase in emission rate (mean 33 μmol m^{-2} d^{-1}) should probably be considered as an extreme case.

As described in the previous section, we use in the standard simulation a DMS oxidation rate which is twice as fast as the reactions with OH and NO_3 combined. Figure 3b shows that the

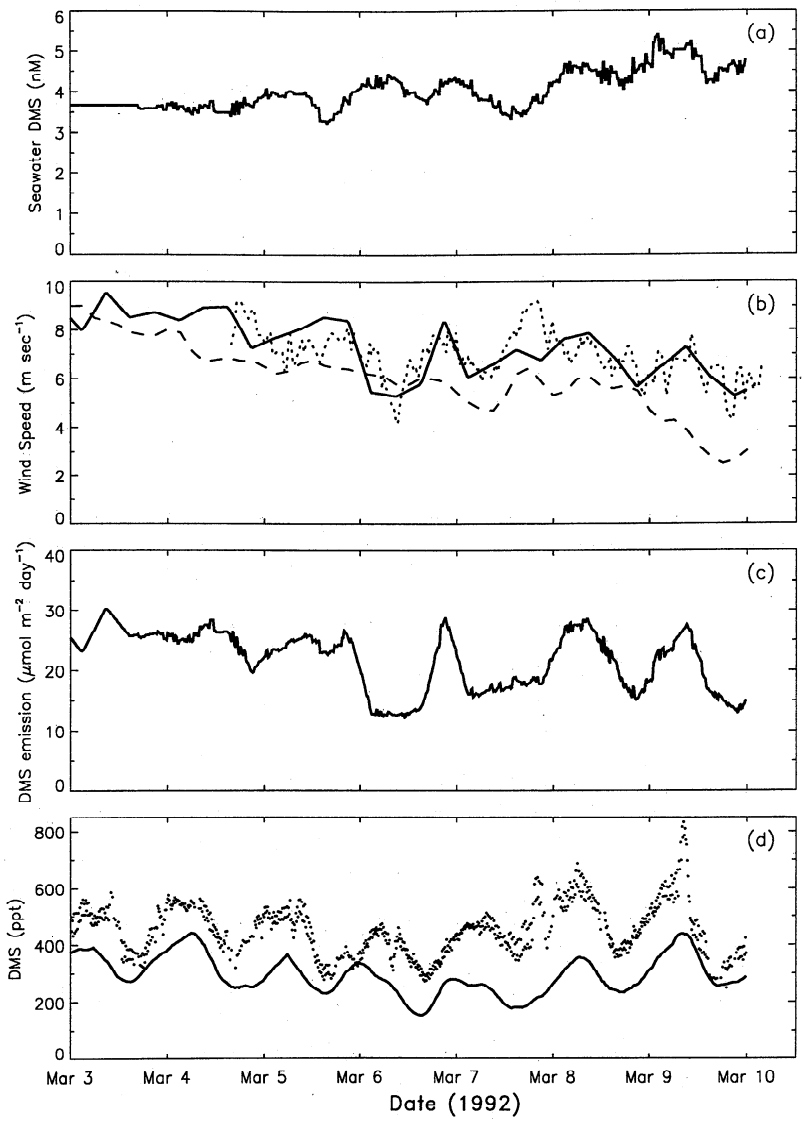

Figure 2. Model input and results of DMS simulations for measurements at a tropical Pacific Ocean site (12°S, 135°W) during March 3–10, 1992: (a) observed seawater DMS concentrations used in the model; (b) 10-m winds from SSM/I (solid line), from GEOS-1 DAS (dashed line), and measured on-site (dotted line); (c) calculated DMS emission rates in the model using the seawater DMS in Figure 2a and SSM/I winds in Figure 2b; and (d) observed (dots) and calculated (line) surface air DMS concentrations.

surface DMS concentration increases 70% from the standard simulation when the DMS oxidation rate is not doubled. However, as discussed below, without a factor of 2 increase in DMS oxidation rate, the modeled amplitude of DMS diurnal variation is a factor of 2 too small compared to the observations.

A typical radiosonde profile from the station showed a mixed layer height of about 60 mbar above the surface [*Yvon et al.*, 1996], but the boundary layer height in the GEOS-1 DAS was between 100 and 200 mbar above the surface at the station. To simulate a reduced boundary layer mixing, we first use a mixing parameter α of 0.15, which is a factor of 2 smaller than the value used in the standard run. Figure 3c shows that the calculated DMS level increases 50% from the standard simulation. Second, the boundary layer height is reduced by a factor of 2, which causes a DMS concentration increase only by 23%, as shown in Figure 3d. These results indicate that the surface concentrations are more sensitive to the variation of α than the boundary layer height in this case.

Another way to reduce the vertical mixing is to suppress the cloud mixing in the model. Convective cloud transport in the model occurs most of the time in the 7-day period above the station, with the strongest cloud mass flux on the last day (March 9). By contrast, the weather condition during the observation period was reported to be generally sunny and clear, with only a few clouds and rain showers [*Yvon et al.*, 1996]. Therefore it seems that the strength of cloud convection at this location may be too strong in the standard run. It has been found in an evaluation of GEOS-1 DAS clouds with data from the International Satellite Cloud Climatology Project (ISCCP) that the GEOS-1 DAS seems to overestimate the amount and spatial coverage of tropical deep convective clouds [*Allen et al.*, 1997]. The ISCCP cloud coverage data for March 3–9, 1992

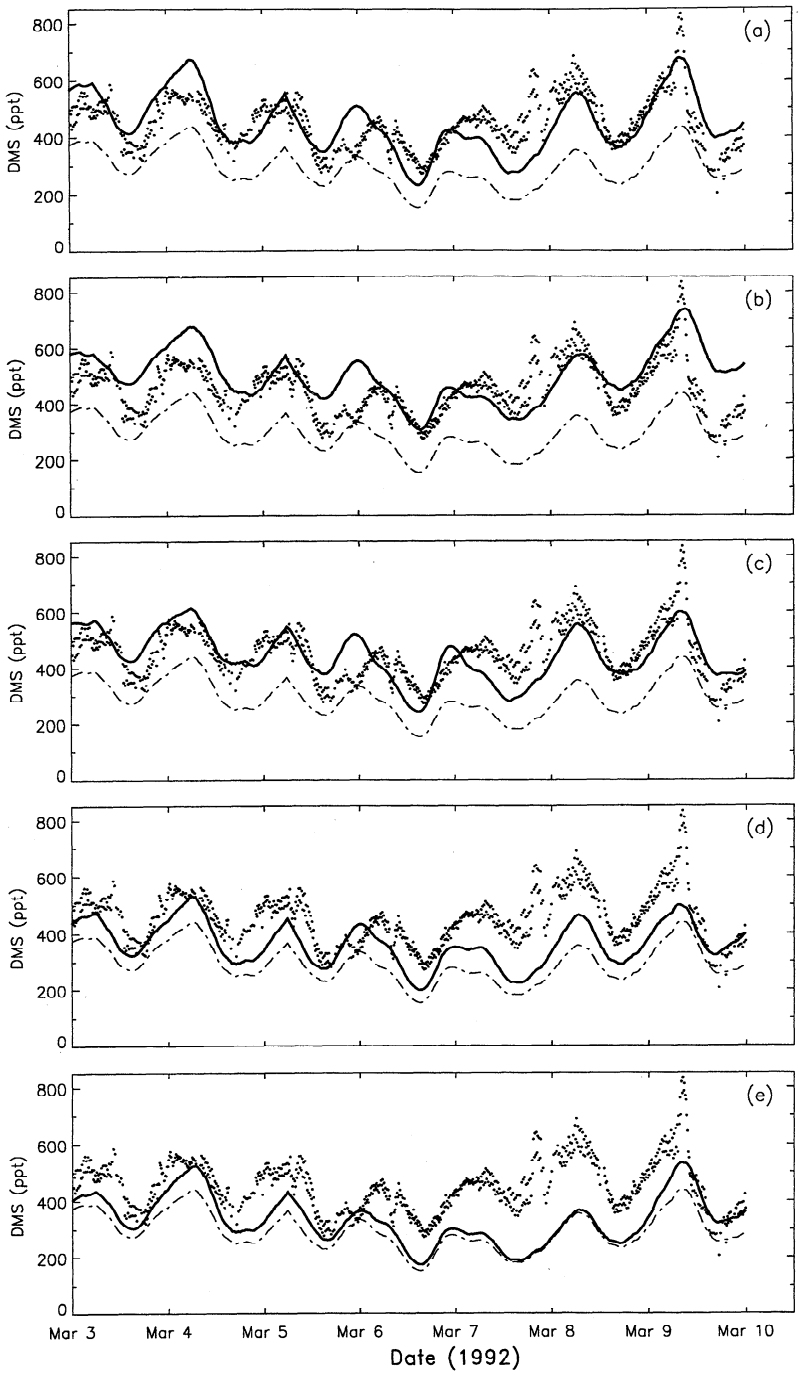

Figure 3. Sensitivity of DMS concentrations to the variations of parameters used in the standard simulation for the site and time period specified in Figure 2: (a) emission rate increased by a factor of 1.6, (b) oxidation rate decreased by a factor of 2, (c) boundary layer mixing parameter α reduced to 0.15, (d) boundary layer height divided by 2, and (e) no deep convective clouds. Results from the standard run are shown in dotted-dashed lines, and from the sensitivity runs are shown in solid lines.

(obtained from the Langley Distributed Active Archive Center (DAAC)), indeed show few convective clouds over this area, contrary to the GEOS-1 DAS cloud diagnostics. We have tested the sensitivity of DMS to the cloud convection in a simulation assuming no convective cloud mixing, and the results are shown in Figure 3e. In this case the surface DMS concentrations on the average are about 14% higher than in the standard simulation but are 20–25% higher on March 4, 5, and 9, when the cloud mass fluxes in the model are more intensive.

Considering the differences between observed and GEOS-1 DAS meteorological conditions, we conduct a simulation by using more "realistic" meteorological values. In this simulation, 10-m winds were from the real-time local observations (Figure 2b), while boundary layer height was reduced to half of

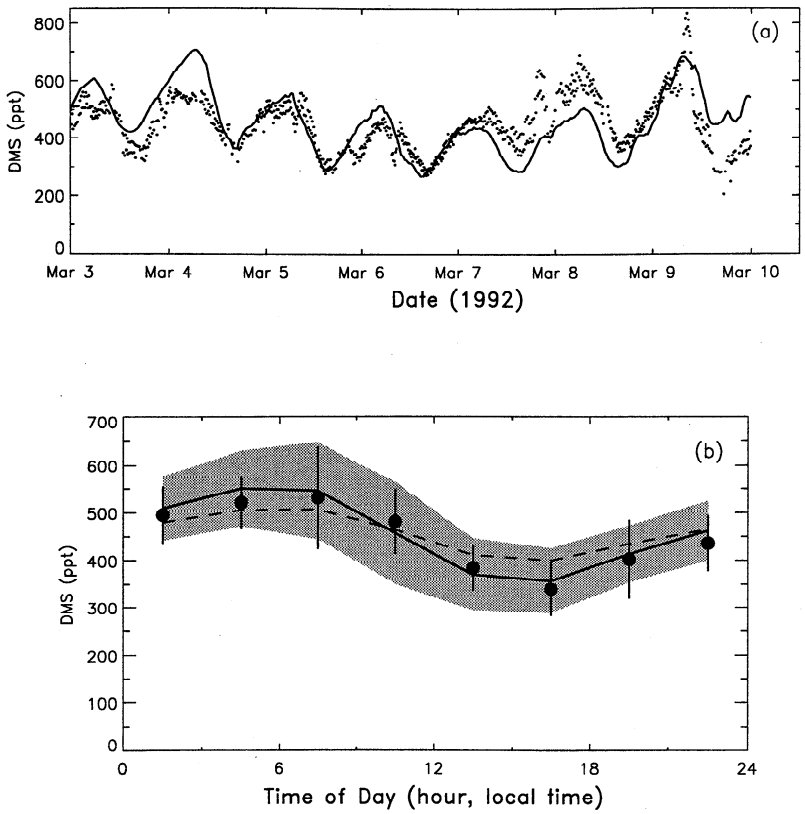

Figure 4. Simulation of DMS for the site and time period specified in Figure 2 assuming no convective cloud mixing, reduced boundary layer height (half of its original value), and using locally observed 10-m winds for calculating DMS emission: (a) time series of observed (dots) and calculated (line) surface air DMS concentrations and (b) observed and simulated DMS diurnal variations averaged in 3-hour bins. Observations are shown by solid circles, with standard deviation in 3-hour bins shown in vertical lines across the symbol. Model results are shown by the thick line, with standard deviation in 3-hour bins shown in the shaded area. Dashed line is a simulation without a factor of 2 increase in the rate of DMS oxidation, normalized to the average DMS shown by solid line.

its original value; furthermore, no cloud convection was taken into account. Results from this simulation are shown in Figure 4. The model reproduces the observed daily average DMS concentrations to within 17%, and diurnal variations to within 5%. Both the observations and the model show an early morning maximum and a late afternoon minimum with an amplitude of the diurnal variation (defined as the difference of the maximum and the minimum divided by the mean values) being approximately 20%; this variation is regulated by the rate of DMS reaction with OH. It should be noted that only when the reaction rate of DMS + OH in the model is increased by a factor of 2 can the amplitude of DMS diurnal variation be reproduced. This is further demonstrated in Figure 4b, where the dashed line represents the results from a simulation without a factor of 2 increase in DMS oxidation rate (DMS concentrations are normalized to the mean value of 457 ppt from the previous run). Without the factor of 2 increase in DMS oxidation rate, the amplitude of DMS diurnal variation is only 11%. This is consistent with the conclusion from *Yvon et al.* [1996] in a box model calculation.

3.2. DMS Across the Tropical South Atlantic (Case 2)

The atmospheric and seawater DMS concentrations across the tropical South Atlantic were measured on the research vessel *Meteor* during February–March 1991 [*Andreae et al.*, 1994, 1995; *Suhre et al.*, 1995]. Most of the cruise track was along 19°S latitude, proceeding from oceanic regions with low productivity (off the coast of Brazil) and low seawater DMS concentrations to regions with higher productivity (upwelling region off the Africa coast) and higher seawater DMS concentrations (Figure 5a). The observed seawater DMS concentrations were used in the model along the cruise track. The 10-m winds from SSM/I for calculating DMS emission again more closely resemble the measured wind speeds than the GEOS-1 DAS 10-m winds (Figure 5b). The calculated DMS emission rates are below 10 μmol m^{-2} d^{-1} for February but are significantly higher for March, ranging from 10 to 50 μmol m^{-2} d^{-1} (Figure 5c). The calculated atmospheric DMS concentrations are compared with the observations in Figure 5d. The increase in DMS concentrations with eastward longitude is captured by the model, but DMS concentrations on average are overestimated by more than a factor of 2. The difference is especially pronounced during the period of March 11–16, when the average DMS in the model is a factor of 3.4 higher than in the observations.

To explain the discrepancies between the observed and calculated DMS concentrations, we have conducted several sensitivity studies where, as in case 1, the rates of DMS emission

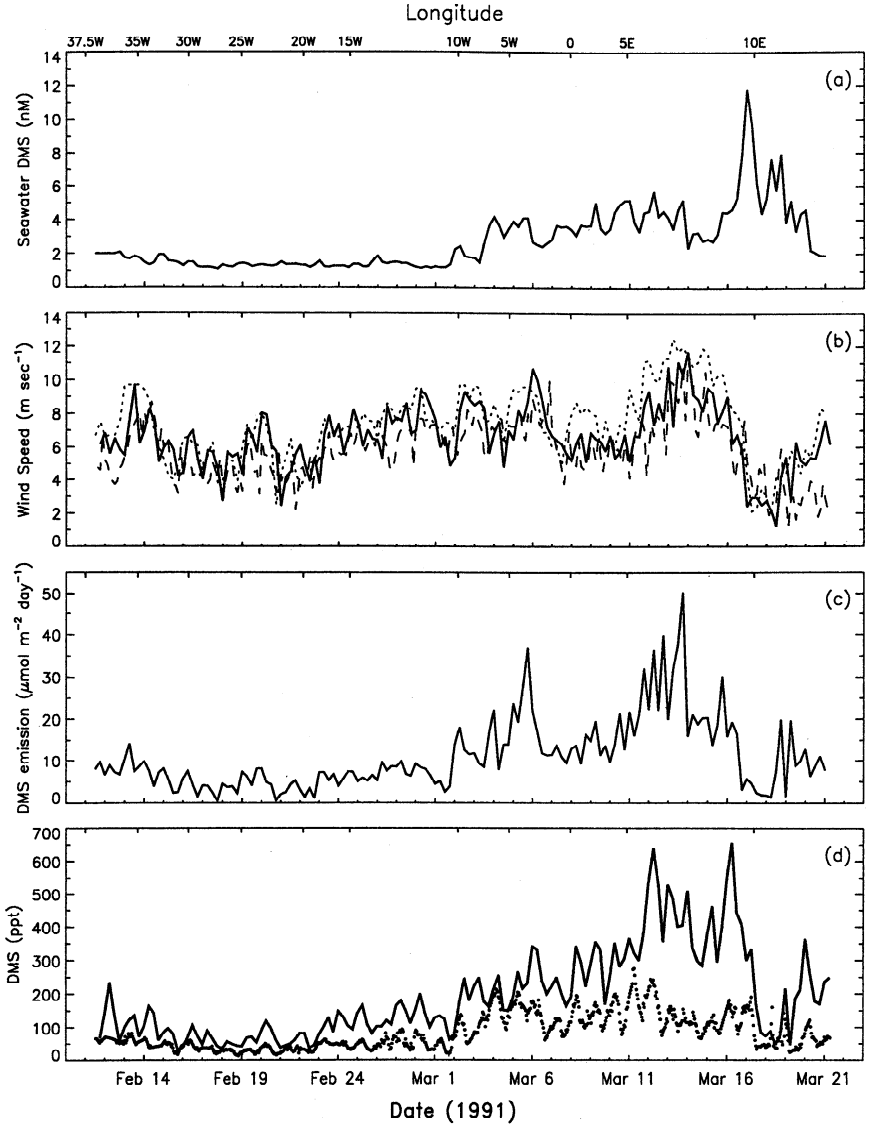

Figure 5. Model input and results of DMS simulation for tropical Atlantic ship cruise measurements along 19°S from February 11 to March 21, 1991: (a) observed seawater DMS concentrations used in the model, (b) 10-m winds from SSM/I (solid line), from GEOS-1 DAS (dashed line), and measured on-site (dotted line), (c) calculated DMS emission rates in the model using the seawater DMS in Figure 5a and SSM/I winds in Figure 5b, and (d) observed (dots) and calculated (line) surface air DMS concentrations. The longitude corresponding to the observation time is indicated in the top axis.

and oxidation and the strengths of boundary layer mixing and cloud transport are varied. The results are shown in Figure 6.

As indicated in Figure 1, there could be a factor of 2 or more difference in DMS emission rates resulting from the different assumptions about the relationship between the wind speed and the sea-to-air transfer velocity. For example, at wind speeds of 5–12 m s^{-1}, the transfer velocities calculated from the algorithms of *Liss and Merlivat* [1986] and *Wanninkhof* [1992] are only 35–43% and 60–70%, respectively, of the values in the standard simulation. Figure 6a shows the results from a simulation in which the algorithms of *Liss and Merlivat* [1986] is used for calculating DMS emission. Now the agreement between the model and observations is improved drastically: the calculated overall average DMS concentration agrees with the measured value to within 6%. As for the period of March 11–16, the modeled DMS level is now only about 60% higher than in the observations.

Figure 6b presents the results from a simulation where the DMS oxidation rate is doubled from the standard run. The modeled DMS concentrations are reduced by 30% from the standard simulation on the average, but they are still a factor of 2.5 higher than the observed DMS concentrations in the period of March 11–16. Note that the increase of DMS oxidation rate here is actually a factor of 4 increase from the rate of DMS reaction with OH and NO_3; it would be acceptable only if there were major errors in DMS reaction rate coefficients or in OH and NO_3 concentrations calculated from photochemical models, or there were a predominant "missing" DMS oxidant.

Plotted in Figures 6c and 6d are results from simulations where boundary layer mixing is increased. The boundary layer

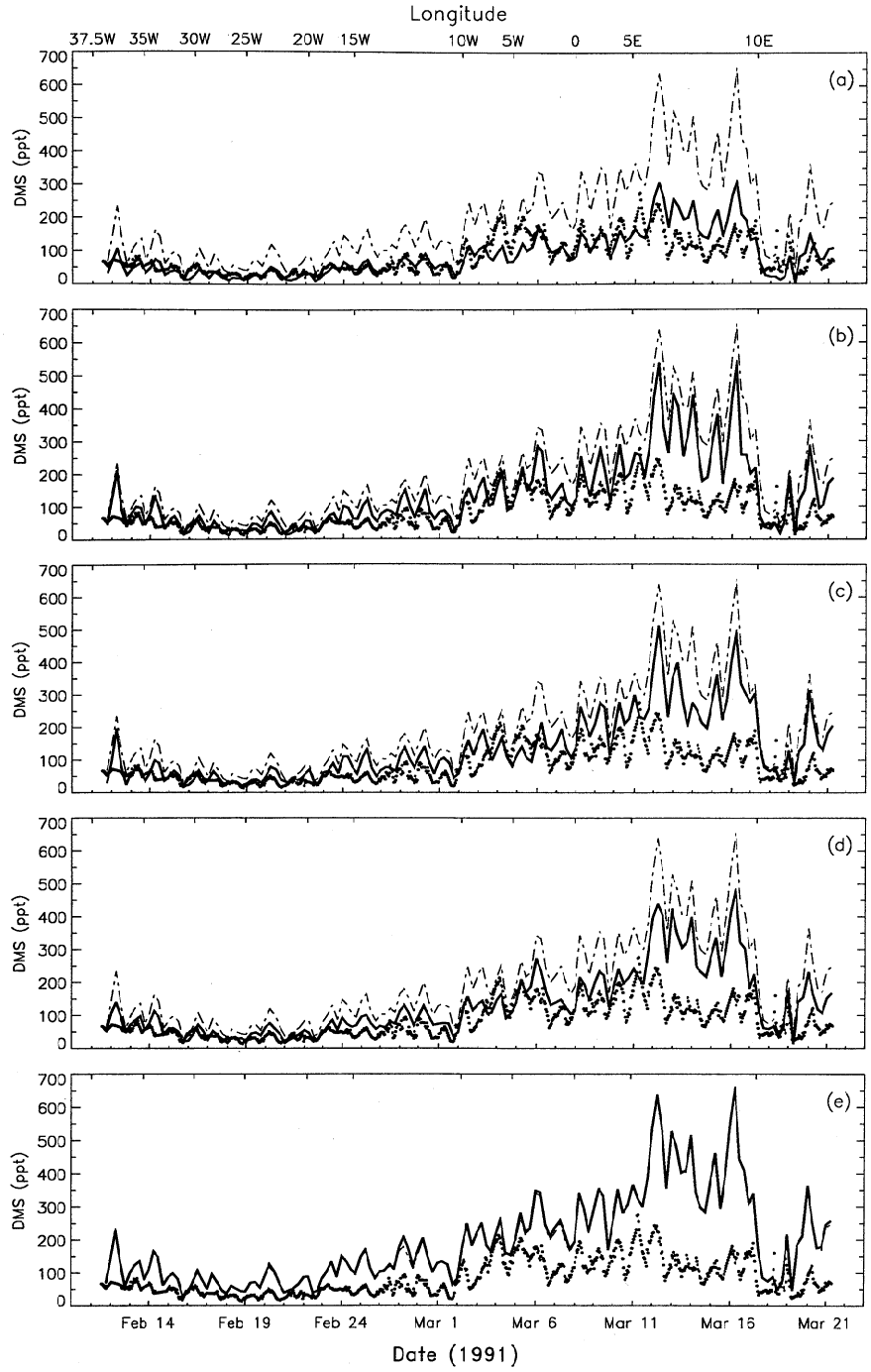

Figure 6. Sensitivity of DMS concentrations to the variations of parameters used in the standard simulation for the site and time period specified in Figure 5: (a) emission rate calculated form the algorithm of *Liss and Merlivat* [1986]; (b) oxidation rate increased by a factor of 2; (c) boundary layer mixing parameter α increased to 1.0; (d) boundary layer height multiplied by 2; and (e) no deep convective clouds. Results from the standard run are shown in dotted-dashed lines, and from the sensitivity runs are shown in solid lines.

height in the GEOS-1 DAS is typically between 100 and 150 mbar above the surface west of 0° longitude (February 11 to March 7), but it reduces to less than 50 mbar east of 0° longitude (after March 7). However, the height of the temperature inversion from the radiosonde soundings taken along the ship track was typically a factor of 2 higher than the boundary layer height in the GEOS-1 DAS; thus the boundary layer mixing is probably underestimated in the standard simulation. To increase the boundary layer mixing, we use a boundary layer mixing parameter α of 1.0 in the first experiment (Figure 6c), and double the boundary layer height in the second one (Figure 6d). The responses of surface air DMS concentrations are very similar in these two experiments, i.e., DMS concentrations are reduced about 30% from the standard simulation.

When the cloud mixing is turned off in the model, as illustrated in Figure 6e, the calculated surface DMS concentrations

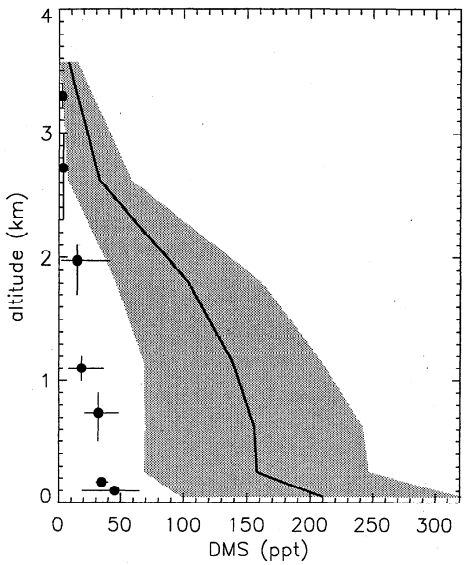

Figure 7. Vertical profile of DMS off Tasmania near Cape Grim (41°S, 145°E). Observations (solid circle) are daytime values averaged over seven vertical bins for the period of December 8–17, 1986. The ranges of observed DMS are shown by horizontal lines across the solid circles, and the extent of the seven vertical bins is shown by vertical lines across the solid circles. Model results (solid line) are daytime average values for the sampling period with standard deviation (1σ) shown in the shaded area.

are only on the average 2% higher than those in the standard simulation. This is because the cloud convective process in the model is weak, especially after March 7, where there are no cloud mass fluxes in the GEOS-1 DAS for the cruise region. Inspection of ISCCP cloud coverage (from Langley DAAC) confirms that there were no deep convective clouds along the path of the cruise after March 7 (east of 0° longitude). Therefore boundary layer mixing is the major process governing the vertical mixing process in this case.

These sensitivity studies suggest that the overestimation of DMS emission rates is probably the main reason for DMS concentrations being too high in the standard simulation. Results from this and the previous (Pacific station) case have shown that there is no simple universal relationship between 10-m wind speed and transfer velocity. While the higher value of transfer velocity from the *Tans et al.* [1990] algorithm best describes the DMS emission rate in the tropical Pacific station in case 1, the lower value from the *Liss and Merlivat* [1986] algorithm seems to better explain the observed DMS concen-

over the period of December 8–17, 1986. Observations were from aircraft measurements with a sampling time of 15–60 min [*Berresheim et al.*, 1990]. The data shown in Figure 7 are averaged over the sampling period and in seven altitudinal bins. The "default" seawater DMS concentration of 1–2 nmol L^{-1} was used in the model. Since there were no SSM/I observations before July 1987, the 10-m winds in the GEOS-1 DAS were used to calculate DMS emission. However, average GEOS-1 10-m wind in December for this region is below 3 m s^{-1}, which is more than a factor of 2 lower than both the reported surface wind speed (2–12 m s^{-1}) [*Berresheim et al.*, 1990] and the 8-year record of SSM/I 10-m winds in December (5.3 m s^{-1}) for the same region. We therefore scaled the GEOS-1 10-m winds to the 8-year average December 10-m wind speed from SSM/I for calculating DMS emission.

The modeled DMS vertical concentrations (solid line in Figure 7) are more than 4 times higher than the measured data. The measured DMS in the marine boundary layer shown in Figure 7 is 15–60 ppt, which is much lower than previous surface air DMS measurements in the same season at Cape Grim (mean 125 ppt [*Andreae et al.*, 1985]; mean 160 ppt [*Ayers et al.*, 1991]). The dominant meteorological feature during the field measurements was the strong subsidence after the cold front [*Berresheim et al.*, 1990], which brought free tropospheric air with low DMS concentrations to lower altitudes. But the calculated concentrations are representative of average values over the grid scale, rather than the values immediately behind cold fronts as in the measurements, which perhaps experienced more intense subsidence on a subgrid scale.

Other possible explanations for modeled DMS being too high include that the calculated DMS emission rate is too high or the DMS loss rate is too slow. Figure 8a plots the results from three sensitivity studies. Using the sea-to-air transfer velocity of the *Liss and Merlivat* [1986] algorithm, the calculated DMS concentration is about 25% lower than in the standard simulation, but it is still 3 times higher than in the observations. Doubling the DMS oxidation rates from the standard run causes the same factor decrease of DMS concentration in the vertical column, although the results are still a factor of 2 too high. The combination of using Liss and Merlivat emission and fast loss rate results in a DMS vertical profile which reproduces the observations within their standard deviation range; the calculated mean value is only 20–40% higher than the observed DMS profile. However, as has been pointed out in the sensitivity tests in case 2 (cross Atlantic), this fast DMS loss rate is a factor of 4 increase from the rate of DMS reaction with OH and NO_3 and is difficult to justify.

The sensitivity of the DMS vertical profile to the vertical

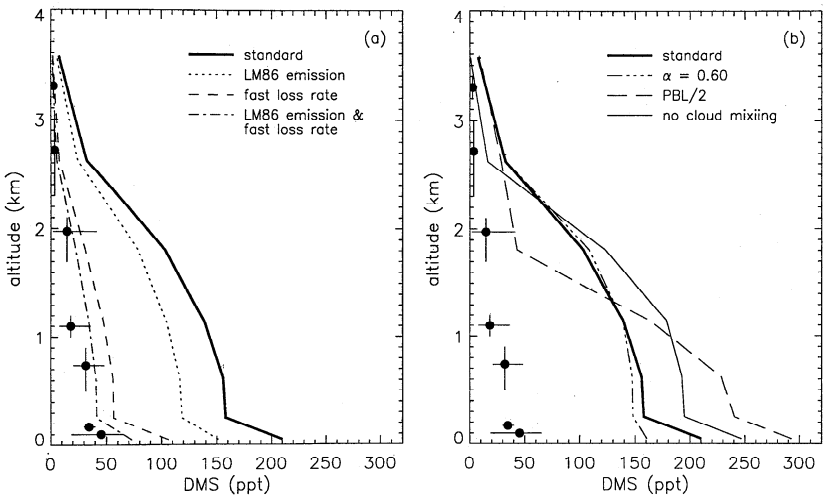

Figure 8. (a) Sensitivity of DMS vertical distributions to the change of the emission algorithm (LM86 is emission algorithm from *Liss and Merlivat* [1986]), oxidation rate (fast loss rate: a factor of 2 increase from the standard run), and the combination of using LM86 and fast loss rate. (b) Sensitivity of DMS vertical distributions to the change of boundary layer mixing parameter α, boundary layer height, and cloud mixing. The site and time period are specified in Figure 7. Observations shown in Figure 7 are also plotted.

are sensitive to the change of DMS emission or oxidation rates but the DMS profile is not. On the other hand, variation of cloud mixing will redistribute DMS throughout the vertical column, while the boundary layer mixing process has an impact mainly on DMS concentrations in the lower troposphere.

3.4. Summertime DMS at Amsterdam Island (Case 4)

Daily concentrations of DMS at 0630 local time measured at Amsterdam Island in the southern Indian Ocean (37.8°S, 77.5°E) have been reported for two austral summer seasons, December 1989 to January 1990 and December 1990 to January 1991 [*Putaud et al.*, 1992]. The observations are shown in Figure 9 together with model results at 0500 local time. We used in the model the monthly average seawater DMS concentrations of 1 nmol L^{-1} measured at Amsterdam Island for these two summers [*Nguyen et al.*, 1992]. The tendency of the day-to-day DMS fluctuation is predicted by the model, although the magnitude of this fluctuation is usually smaller in the model than in the observations. It is expected that the model would underestimate the DMS variations here, since there is essentially no temporal variation of seawater DMS concentrations in the model for the

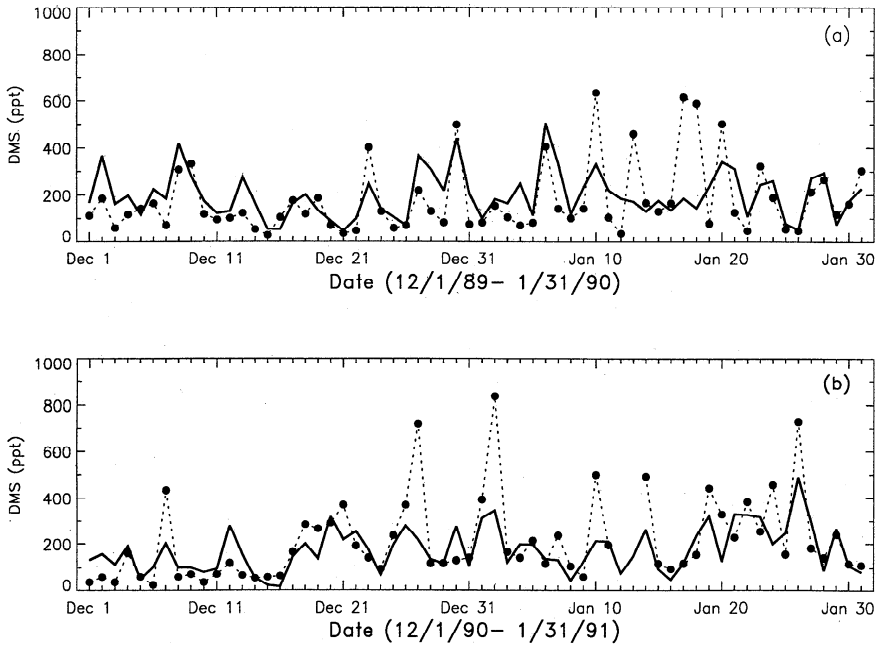

Figure 9. Daily variation of observed (solid circles with dashed line) and simulated (solid line) early morning DMS at Amsterdam Island (37.8°S, 77.5°E) for the period of (a) December 1, 1989 to January 31, 1990 and (b) December 1, 1990 to January 31, 1991.

entire 2 months. The modeled day-to-day fluctuations of DMS are mainly driven by the variations in the 10-m winds which determine the DMS emission rates.

Figure 9 also shows that the model is able to simulate the interannual variability of DMS concentrations. For example, both observation and model show that there is a DMS peak on December 23–24, 1990, reaching a concentration of 300–400 ppt, and yet a valley with a concentration of 100 ppt for the same period in 1989, and the variations of DMS in January 1990 and in January 1991 are basically out of phase. The DMS concentrations in the two summers are not correlated in either observation (correlation coefficient −0.05) or model (correlation coefficient −0.07). The difference in DMS daily variation in the model for the two austral summers is brought about by the variations in 10-m wind speeds (which determine the DMS emission rates) and in vertical mixing, since the seawater DMS concentrations and the oxidation fields used in the model for the two summers are identical.

4. Discussion

From the results of the case studies shown in the previous section, we find that although the model captures many important features of the spatial and temporal variations of DMS concentrations, there are several problems in the model which pose large uncertainties in interpreting the observed DMS levels.

The DMS emission rate is crucial for predicting atmospheric DMS levels and daily variations. Unfortunately, there is no widely available method to measure the DMS emission rate directly. It is typically assumed that the DMS emission rate is dependent on seawater DMS concentration and wind speed. It has been demonstrated in case 1 (tropical Pacific station) and case 2 (Atlantic ship cruise) that it is difficult to use wind speed alone to determine the sea-to-air transfer velocity. New evidence shows the effect of sea surface organic films in reducing gas transfer [*Frew*, 1997]. Although surface-active organic materials are omnipresent at the sea surface, their density and properties vary as functions of biological activity and physical removal processes. Pollution may introduce additional surface-active compounds, particularly in coastal regions and along well-traveled shipping routes (A. Watson, personal communication, 1997). This implies that even under constant physical conditions, transfer velocity may vary as a function of biological processes and pollutant sources, so that in the less productive, cleaner open ocean regions, higher transfer coefficients would be expected than in the biologically more active and often more polluted shelf, coastal, and upwelling regions. These considerations, however, do not necessarily increase the uncertainty range (more than a factor of 2) of the calculated transfer velocity at a given wind speed, as this uncertainty is already reflected in the range of variation of the experimental observations and empirical parameterizations. Rather, they invalidate the assumption that there is a single, "correct" parameterization of transfer velocity based on wind speed alone.

In addition to the uncertainties in calculating DMS transfer velocity, the current seawater DMS database in the model is inadequate, since it has only two seasons with almost no longitudinal dependence. This "default" seawater DMS database must be used at all locations where measurements are unavailable. A better seawater DMS distribution map with spatial resolution of $1° \times 1°$ for every month, based on numerous seawater DMS measurements at different locations and different times of the year, has recently been constructed [*Kettle et al.*, 1996] and will be used in our future simulations.

Our ability to simulate the physics of boundary layer mixing is limited by the model's current parameterization, which chooses a fraction (α) of material to be mixed within the boundary layer. The problem is that α, which should reflect the boundary layer turbulence, is a specified and fixed quantity for the entire global domain and does not vary with time. We found in our simulation that the DMS concentration in the lowest model layer is particularly sensitive to the value of α, although very few differences occurred at layers above the lowest one, as shown in the simulation of vertical profile of DMS at Cape Grim (Figure 8b). In addition, DMS concentrations in the boundary layer are sensitive to the boundary layer height, especially when convective cloud mass flux is low; however, the boundary layer height in GEOS-1 DAS could be inconsistent with the observations. The boundary layer mixing can be improved in future simulations by using turbulent diffusion coefficients instead of α and boundary layer height. The turbulent diffusion coefficients are a function of turbulent heat flux and wind shear in a 3-D field. Although they were not archived in the GEOS-1 DAS, the turbulent diffusion coefficients can be calculated inexpensively using available GEOS-1 DAS diagnostics [*Takacs et al.*, 1994].

Convective cloud transport is the most important process to transport material emitted at the surface to higher altitudes. It was found in a recent study that the distributions and amount of deep convective clouds in the GEOS-1 DAS do not match satellite observations. The model's deep convective mixing is excessive in tropical regions and varies little from day to day, while midlatitude deep convection is too weak at marine locations [*Allen et al.*, 1997]. As a result, the concentrations of short-lived tracers with surface sources could be overestimated by the model in the upper troposphere but underestimated in the boundary layer in the tropical region, while the reverse would apply at midlatitudes. We have seen at the tropical Pacific station (case 1) that excessive cloud convection in the model could affect the DMS surface concentration by 20–25%. Therefore the occurrence of cloud mixing in the model should be carefully verified with local meteorological data or satellite observations.

Although evaluation of DMS chemistry is not the focus of this study, it is worth mentioning that, as found in several previous studies, the DMS oxidation rates need to be increased by a factor of 2 in order for it to be consistent with the emission rates and concentrations of DMS and its products. One might argue that using lower DMS emission rates (e.g., calculated from the *Liss and Merlivat* [1986] algorithm) and lower DMS oxidation rates (e.g., without a factor of 2 increase) could produce similar DMS levels as in the standard simulation. However, as mentioned earlier, high emission rates are found necessary to produce the sulfate levels measured over the remote ocean on a global scale [*Chin et al.*, 1996], and as shown in case 1, only when a factor of 2 increase of DMS oxidation rate is assumed can the amplitude of DMS diurnal variation be reproduced. The need for a higher DMS oxidation rate can be attributed to the possibility that concentrations of the oxidants used in the model are too low, the reported DMS reaction rate coefficients are too low, or there are unaccounted DMS oxidants or oxidation pathways, such as reactions with Cl, Br, and BrO [*Pszenny et al.*, 1993; *Toumi*, 1994; *Vogt et al.*, 1996], or ozone within clouds [*Lee and Zhou*, 1994]. By contrast, it has been shown that oxidation rates of DMS with model-calculated OH were adequate to explain observed DMS and SO_2 levels on

Christmas Island (tropical Pacific) over a 7-day sampling period in summer [*Bandy et al.*, 1996; G. Chen et al., A study of tropical DMS oxidation chemistry: Comparison of Christmas Island field observations of SO_2 and DMS with model simulations, submitted to *Geophysical Research Letters*, 1997; D. D. Davis et al., DMS oxidation in the equatorial Pacific: Comparison of model simulations with field observations for DMS, SO_2, H_2SO_4(g), MSA(g), MS, and NSS, submitted to *Journal of Geophysical Research*, 1997]. One of the major uncertainties in DMS chemistry in this study is that the prescribed OH and NO_x fields generated under the GISS GCM meteorological conditions may not be compatible with the GEOS-1 DAS meteorological environment. We plan in future simulations to use "on-line" chemistry such that the oxidant fields can be generated under the GEOS-1 DAS meteorological conditions.

These case studies have revealed that the discrepancies between the model and observations on a global domain are not likely to be resolved by altering the parameters homogeneously. As we have shown in the case studies, better agreement is achieved in case 1 if vertical mixing is reduced or emission is increased (Figure 3), but the reverse is true in case 2 (Figure 6). A better evaluation of the model and interpretation of observed DMS levels will require comparing model results with both surface and vertical measurements of DMS and its oxidation products such as SO_2 and sulfate. Such a comparison will provide a more constrained evaluation of model processes such as emission flux, oxidation rate, boundary layer mixing, and cloud convection.

5. Conclusions

We have used a global 3-D model, the GEOS CTM, driven by the GEOS-1 DAS assimilated meteorological data, to analyze the processes controlling atmospheric DMS concentrations over the oceans in four case studies. This is the first work where the observed diurnal cycle, day-to-day fluctuations, and interannual variabilities of DMS are simulated in a 3-D model. This study has shown the strengths and weaknesses of the model, tested the sensitivities of atmospheric DMS concentrations to the physical and chemical parameters in the model, and identified areas where the model could be improved.

Model-calculated diurnal variation and daily average values in DMS concentrations agree with observations at a tropical Pacific station to within 5% and 17%, respectively, when observed seawater DMS concentrations and realistic meteorological conditions are used as input to the model. When following a cruise track across the tropical Atlantic, the model captures the trend of DMS concentration change with longitude and time but overpredicts the DMS level, possibly because the calculated DMS emission rate is too high or the vertical mixing is too weak. Concentrations of DMS in the simulated vertical profile off Tasmania near Cape Grim are more than 4 times higher than the observations, presumably due to the incapability of the model to resolve the subgrid-scale strong subsidence immediately after the passage of a cold front, or the calculated emission rate is too high. The model also simulates day-to-day fluctuations and interannual variations measured at Amsterdam Island, although the magnitude of the fluctuations is underpredicted by the model.

The DMS emission and oxidation rates directly affect atmospheric DMS concentrations. The daily and interannual variation of surface air DMS in the model is largely driven by the variability of the 10-m wind speed, which is a crucial parameter in calculating DMS emission rate in the model. The satellite-measured SSM/I 10-m winds have been shown to capture the features of locally measured winds more accurately than GEOS-1 DAS 10-m winds in all our case studies.

Sensitivity studies have demonstrated that surface layer DMS concentrations are sensitive to the specification of the boundary layer mixing parameter α, but at higher altitudes the concentrations are almost unchanged by the choice of α. Varying the boundary layer height affects the DMS concentrations within the boundary layer and the lower troposphere but not in the free troposphere. In contrast, DMS concentrations at all levels from the boundary layer to the free troposphere are sensitive to the convective cloud mixing, which is the most important model process transporting DMS from the surface to higher altitudes.

The diurnal cycle of DMS shows an early morning maximum and a late afternoon minimum, which is mainly controlled by the reaction rate of DMS with OH. However, this rate has to be increased by a factor of 2 from the calculated value in order to reproduce the amplitude of the diurnal variations. It is possible that the OH concentrations in the model and/or the reported DMS + OH rate coefficient are too low; alternatively, there might be a missing DMS oxidation pathway which, though potentially important, has yet to be identified.

Further evaluation of our understanding of the DMS cycle is limited by several factors. The first is the difficulty in parameterizing DMS emission, as it is oversimplified by assuming that DMS emission is solely controlled by the seawater DMS concentration and the 10-m wind speed with a universal relationship. Since there is no simple means to improve the emission algorithm, a possible range of DMS emission rates and sea surface properties should be considered in future simulations. The second is the simplistic parameterization used in the model for boundary layer mixing, a shortcoming which can be improved in the future by using the turbulent mixing coefficients from the GEOS-1 DAS. The third is the inaccurate representation of the spatial distribution and the intensity of deep convective clouds in the GEOS-1 DAS. This affects not only the boundary layer tracer concentrations but, more important, the tracer concentrations and distributions in the free troposphere where the tracer lifetime is usually longer. Therefore the occurrence of cloud mixing in the model should be carefully verified with other observations, such as local meteorological data or satellite observation. Finally, the chemistry used in the present model is "off-line," such that the prescribed oxidant fields may not be consistent with the GEOS-1 DAS meteorological environment. Our future simulations will use "on-line" chemistry to generate the oxidant fields under the GEOS-1 DAS meteorological conditions. A better evaluation of the model and interpretation of observed DMS levels will require comparing model results with both surface and vertical measurements of DMS and its oxidation products such as SO_2 and sulfate. Such a comparison will provide a more constrained evaluation of model processes such as emission flux, oxidation rate, boundary layer mixing, and cloud convection.

Acknowledgments. We wish to thank Shari Yvon-Lewis for providing her measurement data files and Ken Pickering and two anonymous reviewers for their helpful comments. This work was supported by the Universities Space Research Association Visiting Scientist Program at NASA Goddard Space Flight Center, NASA EOS IDS and ACMAP programs, and the NOAA Climate and Global Change Program.

References

Allen, D. J., R. B. Rood, A. M. Thompson, and R. D. Hudson, Three-dimensional radon 222 calculations using assimilated meteorological data and a convective mixing algorithm, *J. Geophys. Res.*, *101*, 6871–6881, 1996a.

Allen, D. J., P. Kasibhatla, A. M. Thompson, R. B. Rood, B. G. Doddridge, K. E. Pickering, R. D. Hudson, and S.-J. Lin, Transport-induced interannual variability of carbon monoxide determined using a chemistry and transport model, *J. Geophys. Res.*, *101*, 28,655–28,669, 1996b.

Allen, D. J., K. E. Pickering, and A. Molod, An evaluation of deep convective mixing in the Goddard chemical-transport model using ISCCP cloud parameters, *J. Geophys. Res.*, *102*, 25,467–25,476, 1997.

Andreae, M. O., Ocean-atmosphere interactions in the global biogeochemical sulfur cycle, *Mar. Chem.*, *30*, 1–29, 1990.

Andreae, M. O., R. J. Ferek, F. Bermond, K. P. Byrd, R. T. Engstrom, S. Hardin, P. D. Houmere, F. LeMarrec, H. Raemdonck, and R. B. Chatfield, Dimethyl sulfide in the marine atmosphere, *J. Geophys. Res.*, *90*, 12,891–12,900, 1985.

Andreae, M. O., W. Elbert, and S. J. de Mora, Biogenic sulfur emissions and aerosols over the tropical South Atlantic, 3, Atmospheric dimethylsulfide, aerosols and cloud condensation nuclei, *J. Geophys. Res.*, *100*, 11,335–11,356, 1995.

Andreae, T. W., M. O. Andreae, and G. Schebeske, Biogenic sulfur emissions and aerosols over the tropical South Atlantic, 1, Dimethylsulfide in seawater and in the atmospheric boundary layer, *J. Geophys. Res.*, *99*, 22,819–22,829, 1994.

Atlas, R., R. N. Hoffman, S. C. Bloom, J. C. Jusem, and J. Ardizzone, A multiyear global surface wind velocity dataset using SSM/I wind observations, *Bull. Am. Meteorol. Soc.*, *77*, 869–882, 1996.

Ayers, G. P., J. P. Ivey, and R. W. Gillett, Coherence between seasonal cycles of dimethyl sulphide, methanesulphonate, and sulphate in marine air, *Nature*, *349*, 404–406, 1991.

Bandy, A. R., D. C. Thornton, B. W. Blomquist, S. Chen, T. P. Wade, J. C. Ianni, G. M. Mitchell, and W. Nadler, Chemistry of dimethylsulfide in the equatorial Pacific atmosphere, *Geophys. Res. Lett.*, *23*, 741–744, 1996.

Bates, T. S., J. D. Cline, R. H. Gammon, and S. R. Kelly-Hansen, Regional and seasonal variations in the flux of oceanic dimethylsulfide to the atmosphere, *J. Geophys. Res.*, *92*, 2920–2938, 1987.

Benkovitz, C. M., M. T. Scholtz, J. Pacyna, L. Tarrason, J. Dignon, E. C. Voldner, P. A. Spiro, J. A. Logan, and T. E. Graedel, Global gridded inventories of anthropogenic emissions of sulfur and nitrogen, *J. Geophys. Res.*, *101*, 29,239–29,253, 1996.

Berresheim, H., M. O. Andreae, G. P. Ayers, R. W. Gillett, J. T. Merrill, V. J. Davis, and W. L. Chameides, Airborne measurements of dimethylsulfide, sulfur dioxide, and aerosol ions over the Southern Ocean south of Australia, *J. Atmos. Chem.*, *10*, 341–370, 1990.

Charlson, R. J., J. E. Lovelock, M. O. Andreae, and S. G. Warren, Oceanic phytoplankton, atmospheric sulphur, cloud albedo, and climate, *Nature*, *326*, 655–661, 1987.

Chatfield, R. B., and P. J. Crutzen, Sulfur dioxide in remote oceanic air: Cloud transport of reactive precursors, *J. Geophys. Res.*, *89*, 7111–7132, 1984.

Chin, M., and D. J. Jacob, Anthropogenic and natural contributions to tropospheric sulfate: A global model analysis, *J. Geophys. Res.*, *101*, 18,691–18,699, 1996.

Chin, M., D. J. Jacob, G. M. Gardner, M. S. Foreman-Fowler, P. A. Spiro, and D. L. Savoie, A global three-dimensional model of tropospheric sulfate, *J. Geophys. Res.*, *101*, 18,667–18,690, 1996.

Erickson, D. J., III, A stability dependent theory for air-sea gas exchange, *J. Geophys. Res.*, *98*, 8471–8488, 1993.

Feichter, J., E. Kjellstrom, H. Rodhe, F. Dentener, J. Lelieveld, and G.-J. Roelofs, Simulation of the tropospheric sulfur cycle in a global climate model, *Atmos. Environ.*, *30*, 1693–1708, 1996.

Frew, N. M., The role of organic films in air-sea gas exchange, in *The Sea Surface and Global Change*, edited by P. S. Liss and R. A. Duce, pp. 121–171, Cambridge Univ. Press, New York, 1997.

Kettle, A. J., et al., A preliminary global database of sea surface dimethylsulfide measurements and a simple model to predict sea surface dimethylsulfide as a function of latitude, longitude, and month (abstract), *Eos Trans. AGU*, *77*(46), 417, Fall Meet. Suppl., 1996.

Langner, J., and H. Rodhe, A global three-dimensional model of the tropospheric sulfur cycle, *J. Atmos. Chem.*, *13*, 225–263, 1991.

Lee, Y.-N., and X. Zhou, Aqueous reaction kinetics of ozone and dimethylsulfide and its atmospheric implications, *J. Geophys. Res.*, *99*, 3597–3605, 1994.

Lin, S.-J., and R. B. Rood, Multidimensional flux-form semi-Lagrangian transport schemes, *Mon. Weather Rev.*, *124*, 2046–2070, 1996.

Lin, S.-J., W. C. Chao, U. C. Sud, and G. K. Walker, A class of the van Leer-type transport schemes and its application to the moisture transport in a general circulation model, *Mon. Weather Rev.*, *122*, 1575–1593, 1994.

Liss, P. S., and L. Merlivat, Air-sea gas exchange rates: Introduction and synthesis, in *The Role of Air-Sea Exchange in Geochemical Cycling*, pp. 113–127, edited by P. Buat-Ménard, D. Reidel, Norwell, Mass., 1986.

Nguyen, B. C., N. Mihalopoulos, J. P. Putaud, A. Gaudry, L. Gallet, W. C. Keene, and J. N. Galloway, Covariations in oceanic dimethylsulfide, its oxidation products and rain acidity at Amsterdam Island in the southern Indian Ocean, *J. Atmos. Chem.*, *15*, 39–53, 1992.

Pham, M., J.-F. Müller, G. Brasseur, C. Granier, and G. Megie, A three-dimensional study of the tropospheric sulfur cycle, *J. Geophys. Res.*, *100*, 26,061–26,092, 1995.

Pszenny, A. A., W. C. Keene, D. J. Jacob, S. Fan, J. R. Maben, M. P. Zetwo, M. Springer-Young, and J. N. Galloway, Evidence of inorganic chlorine gases other than hydrogen chloride in marine surface air, *Geophys. Res. Lett.*, *20*, 699–702, 1993.

Putaud, J. P., N. Mihalopoulos, B. C. Nguyen, J. M. Campin, and S. Belviso, Seasonal variations of atmospheric sulfur dioxide and dimethylsulfide concentrations at Amsterdam Island in the southern Indian Ocean, *J. Atmos. Chem.*, *15*, 117–131, 1992.

Schubert, S. D., R. B. Rood, and J. Pfaendtner, An assimilated data set for earth science applications, *Bull. Am. Meteorol. Soc.*, *74*, 2331–2342, 1993.

Smethie, W. M., Jr., T. Takahashi, D. W. Chipman, and J. R. Ledwell, Gas exchange and CO_2 flux in the tropical Atlantic Ocean determined from ^{222}Rn and pCO_2 measurements, *J. Geophys. Res.*, *90*, 7005–7022, 1985.

Spiro, P. A., D. J. Jacob, and J. A. Logan, Global inventory of sulfur emissions with $1° \times 1°$ resolution, *J. Geophys. Res.*, *97*, 6023–6036, 1992.

Spivakovsky, C. M., R. M. Yevich, J. A. Logan, S. C. Wofsy, M. B. McElroy, and M. J. Prather, Tropospheric OH in a three-dimensional chemical tracer model: An assessment based on observations of CH_3CCl_3, *J. Geophys. Res.*, *95*, 18,441–18,472, 1990.

Suhre, K., M. O. Andreae, and R. Rosset, Biogenic sulfur emissions and aerosols over the tropical South Atlantic, 2, One-dimensional simulation of sulfur chemistry in the marine boundary layer, *J. Geophys. Res.*, *100*, 11,323–11,334, 1995.

Takacs, L. L., A. Molod, and T. Wang, Documentation of the Goddard Earth Observing System (GEOS) general circulation model–version 1, *NASA Tech. Memo.*, *TM-104606*, vol. 1, 1994.

Tans, P. P., I. Y. Fung, and T. Takahashi, Observational constraints on the global atmospheric CO_2 budget, *Science*, *247*, 1431–1438, 1990.

Toumi, R., BrO as a sink for dimethylsulfide in the marine atmosphere, *Geophys. Res. Lett.*, *21*, 117–120, 1994.

Vogt, R., P. J. Crutzen, and R. Sander, A mechanism for halogen release from sea-salt aerosol in the remote marine boundary layer, *Nature*, *383*, 327–330, 1996.

Wanninkhof, R., Relationship between wind speed and gas exchange over the ocean, *J. Geophys. Res.*, *97*, 7373–7382, 1992.

Yvon, S. A., E. S. Saltzman, D. J. Cooper, T. S. Bates, and A. M. Thompson, Atmospheric sulfur cycling in the tropical Pacific marine boundary layer (12°S, 135°W): A comparison of field data and model results, 1, Dimethylsulfide, *J. Geophys. Res.*, *101*, 6899–6909, 1996.

D. J. Allen, Department of Meteorology, University of Maryland, College Park, MD 20742.

M. O. Andreae, Biogeochemistry Department, Max Planck Institute for Chemistry, 55020 Mainz, Germany.

J. V. Ardizzone, General Sciences Corporation, NASA Goddard Space Flight Center, Greenbelt, MD 20771.

R. M. Atlas, R. B. Rood, and A. M. Thompson, NASA Goddard Space Flight Center, Greenbelt, MD 20771.

M. Chin, NASA Goddard Space Flight Center, Greenbelt, MD 20771. (e-mail: chin@rondo.gsfc.nasa.gov)

S.-J. Lin, JCET, University of Maryland at Baltimore County, NASA Goddard Space Flight Center, Greenbelt, MD 20771.

(Received July 11, 1997; revised January 5, 1998;
accepted January 5, 1998.)